Biochemical and Biophysical Research Communications 520 (2019) 14–19

Contents lists available at ScienceDirect

Biochemical and Biophysical Research Communications

journal homepage: www.elsevier.com/locate/ybbrc

Revealing conformational dynamics of 2′-*O*-methyl-RNA guanine modified G-quadruplex by replica exchange molecular dynamics

Yanrong Ke [a], Hongwei Jin [c], Lidan Sun [b, *]

[a] School of Management, Xiamen University, Xiamen, 361005, China
[b] College of Chemical Engineering and Material Science, Quanzhou Normal University, Quanzhou, 362000, China
[c] State Key Laboratory of Natural and Biomimetic Drugs, School of Pharmaceutical Sciences, Peking University, Beijing, 100191, China

ARTICLE INFO

Article history:
Received 30 August 2019
Received in revised form
8 September 2019
Accepted 16 September 2019
Available online 26 September 2019

Keywords:
2′OMe-G
G-quadruplex
TBA
REMD

ABSTRACT

Thrombin-binding DNA aptamer (TBA) can fold into an antiparallel unimolecular G-quadruplex (G4) structure. Different types of modifications lead to various effects on the structure and stability of the G4 structure. Previous study has shown that a modified TBA (mTBA) that 2′-deoxy guanine (dG) at positions 10 and 11 in the TBA sequence were replaced by 2′-*O*-methyl-RNA guanine (2′OMe-G) can't fold into a well-defined G4 structure. In order to investigate the detailed structural information and probe the instability factors, we successfully employed the replica exchange molecular dynamics (REMD) to characterize the large conformational variations of the mTBA and systemically describe the influences of the 2′OMe-G on the mTBA in terms of conformation variations and the probability distributions of Hoogsteen hydrogen bonds, dihedral, sugar pucker and glycosyl torsion angle. Replacing position 10 with the 2′OMe-G (2′OMe-G10) induced a strong destabilization of the aptamer, while the 2′OMe-G at position 11(2′OMe-G11) was less destabilizing. More importantly, the glycosyl torsion angle and sugar pucker of 2′OMe-G10 were the most critical destabilization factors. These results were in good agreement with the theoretical and experimental results. Moreover, the structure information can be used as guidelines for the further design of modifications on G4 structure.

1. Introduction

DNA and RNA sequence containing guanine rich tandem repeats prone to fold into a variety of stable G-quadruplex (G4) structures that have attracted a lot of interest for their special structural features and important biological functions [1–4]. Typically, G4 is mainly formed by G-quartets and loops which serve to connect together the G-quartets. G-quartet is constituted by four coplanar guanines that associate via eight Hoogsteen hydrogen bonds [5]. The highly electronegative channel is stabilized by monovalent metal cations, such as K^+ or Na^+, located between two adjacent G-quartets [6,7].

The most studied aptamer, thrombin-binding DNA aptamer (TBA), with a consensus 15-base sequence, d(GGTTGGTGTGGTTGG), has been shown to inhibit thrombin-catalyzed fibrin clot formation in vitro [8]. X-ray experiments showed that TBA can fold into an unimolecular antiparallel G4 consisting of two G-quartets connected by two TT loops and one TGT loop when bind to thrombin protein with good specificity and high affinity [9,10]. To improve the properties of TBA, many modifications associated with TBA have been reported thus far, including LNA, 2′-*O*-methyl-RNA guanine (2′OMe-G), D-/L-Isonucleoside, unlocked nucleic acid [11–14]. Albeit many different strategies have been reported, these modifications displayed different roles: either promote or destroy the formation of G-quadruplex with a strong position and number dependent fashion.

Probing details of the G4 structures can provide numerous of useful information for theoretical and application research. Many experimental methods have been utilized to capture and detect these complicated processes, such as Single-molecule Fluorescence resonance energy transfer (smFRET), UV, surface plasmon resonance (SPR), NMR and CD [15–18]. Molecular dynamics (MD) simulation has been successfully applied for the simulations of nucleic acid structures and this computational tool has provide valuable information that is not experimentally accessible [19–21].

Abbreviations: TBA, Thrombin-binding DNA aptamer; dG, 2′-deoxy guanine; 2′OMe-G, 2′-*O*-methyl-RNA guanine; REMD, replica exchange molecular dynamics; G4, G-quadruplex; RMSD, Root mean-square deviation.

* Corresponding author.
E-mail address: sld85@126.com (L. Sun).

https://doi.org/10.1016/j.bbrc.2019.09.065
0006-291X/

In case of classical MD, a conformational search is carried out by random walk in energy space, whereas replica exchange molecular dynamics (REMD) performs random walk in temperature space followed by the same in configuration space. In other words, REMD simulation allowed significantly improving sampling of conformational space by simulating different replicas of the system at different temperatures and swapping between them [22]. Obviously, the exchange from low to high temperatures prevents the system from getting trapped in one of the several local minimas. Recently, REMD has been used to probe unfolding process of TBA and has provided valuable insights into early unfolding and late folding events [23,24].

In our previous study, we have successfully investigated the structural characteristics of several TBAs modified with LNA, D-/L-Isonucleoside, 2′OMe-G by MD simulation [25,26]. In addition, Guan et al. has showed that the modified TBA (mTBA) that both 2′-deoxy guanine at positions 10 and 11 of the TBA were replaced by 2′OMe-G by CD and UV experiments which has proved that the modified sequence can't fold into a well-fined G4 structure [12]. It is well known that the large conformation variation of G4 structure is a rather slow process and due to the limitation of conformational sampling, it is hard to simulate the large conformation of G4 structure by classical MD simulation and the detailed structural information is insufficient. In order to overcome this deficiency, for the first time we successfully employed the REMD method to simulate the conformation variations of the mTBA and investigate the detailed effects of the 2′OMe-G substitutions on the G4 structure.

By analyzing the clustering analysis of sampled conformations, distributions and relationships of the structural parameters such as Hoogsteen hydrogen bonds, dihedral, sugar pucker and glycosyl torsion angle, we systematically revealed that the two substitutions displayed different implications of the mTBA: the 2′OMe-G10 replacement induced a strong destabilization of the aptamer, while the 2′OMe-G11 was less destabilizing. Moreover, the detailed structural analysis indicated the glycosyl torsion angle and sugar pucker contributed to the most destabilization effects on the mTBA. These conclusions are in agreement with the theoretical and experimental results and indicate that REMD can be used to inquire on the large conformation variants of G4 structures. Furthermore, these results provide insights into the structural dynamic variations of mTBA and can be used as guidelines for the design and modifications of G4 structure.

2. Method

The simulations were performed using the AMBER 11 suite of programs over total simulation time of 25 ns per replica. The starting structure was prepared by obtaining the NMR structure of TBA (PDB entry 1C35) and the following modifications, 2′OMe-G10 and 2′OMe-G11, were built using LEaP module. In total, 8 replicas were simulated with the following simulation temperatures (in Kelvin): 300.0, 310.0, 321.0, 334.0, 353.0, 375.0, 397.0, and 420.0. These simulation temperatures were selected to give approximately uniform acceptance ratios for exchanges between neighboring replicas [27]. The 2′OMe-G force field parameters weren't developed in AMBER and we downloaded these from the amber website (http://ambermd.org/). ff99SB force field and generalized Born (GB) solvation model were applied to describe the G4 structure and the solvation effect, respectively. An integration time step of 2 fs was used. The resulting system was minimized with the steepest descent method followed by 1 ns of simulation for each replica slowly heating them to their respective temperatures using a Langevin thermostat. At last, the REMD simulations were conducted for 25 ns of each replica at their own temperatures. Ptraj module of Amber was used to perform the root mean square deviation (RMSD) calculations, cluster analysis, Hoogsteen hydrogen bonds, dihedral, sugar pucker and glycosyl torsion angle. The Stata software was used to compute the probability distributions. Discovery studio and pymol were used to visualize the structure and trajectories.

3. Results and discussion

3.1. Convergence of simulations

REMD simulations of mTBA resulted in generation of 8 trajectories one for each replica and the total simulation time is 200 ns To characterize atomic fluctuation and the convergence during the course of MD simulations, the RMSD fluctuation was calculated and the initial NMR structure as a reference for computing the RMSD values. We calculated the RMSD (calculated without the K+ ions) during the production run at 300 K and 375 K. As shown in Fig. 1A and B, the two RMSD curves suggested that the simulation produced stable trajectories to enable collection of snapshots for further analysis. With respect to the initial model, the RMSD values are over 10 Å, which is an indication of the large conformation variations of the mTBA.

3.2. Clustering analysis

Clustering analysis can detect and classify objects into different groups based on structural similarity. The structures from all the 8 trajectories were clustered by setting RMSD criterion for the modified structure to probe the possible intermediate structures in the unfolding progress. The entire REMD trajectories were divided into five clusters and the representative structures of the three most populated clusters were shown in Fig. 1C, D and E. The first cluster (62.5%) showed that the two well-defined G-quartets totally lost the hydrogen bond interactions, especially for the terminal guanines. It has been demonstrated that the terminal guanines interactions are necessary for the folding process and stability [24]. The second cluster displayed a propensity of 12.5% with the two G-quartets were totally divided into two parts, but some local base stacking interactions were still existed. Interestingly, this phenome is also observed in the NMR experiment and our previous SMD simulation results, and these structural characteristics are elucidated as the possible intermediate structures necessary for the folding process of TBA [24]. The third cluster (17%) had formed an unfolding state just behaving similar to a random coil. Obviously, the clustering analysis results of the REMD trajectories suggested that mTBA has lost the critical structural characteristics of G4 and can't exist as a stable G4 structure, which are in good agreement with previous experimental results [12]. More importantly, the disruption process of the mTBA G4 structure can provide numerous structural information and help us to understand the critical destabilization factors.

3.3. Hoogsteen hydrogen bonds analysis

An important descriptor of the stability and constructed situation of G4 structure is the Hoogsteen hydrogen bonds formed by the two G4-quartets. We computed the existence percentages of Hoogsteen hydrogen bonds during the production run to demonstrate the stability of the two modified G4-quartets. As shown in Table 1, we observed that only partly hydrogen bonds were formed and the values of percentage occupancy dramatically decreased with the best situation is 49.64%. Compared to the second G4-quartet-B (dG2, dG5, 2′OMe-G11 and dG14), the first G4-quartet-A (dG1, dG6, 2′OMe-G10 and dG15) was more unstable with the

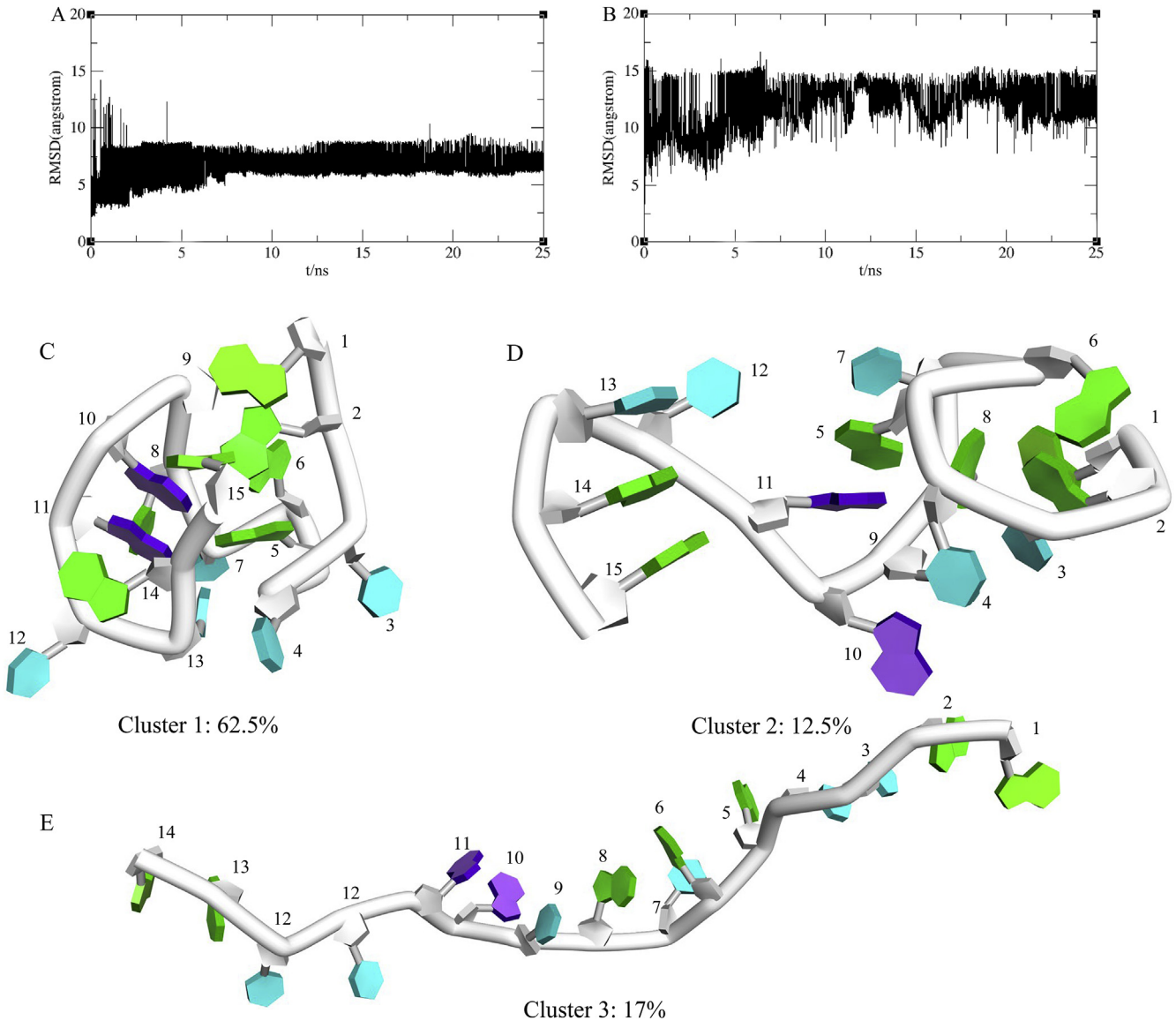

Fig. 1. The RMSD curves of mTBA at 300 K(A) and 375 K(B) and the representative structures of the three most populated clusters (C, D and E). The purple represents 2′OMe-G, the green represents dG and the cyan represents dT. (For interpretation of the references to colour in this figure legend, the reader is referred to the Web version of this article.)

Table 1
The Hoogsteen hydrogen bonds formed by the eight guanines during the REMD simulations.

Hydrogen bonds between nucleo-bases (G4-quartet-A)		% Population	Hydrogen bonds between nucleo-bases (G4-quartet-B)		% Population
dG15@O6	OMe-dG10@N1	23.9	OMe-dG11@N7	dG14@N2	42.36
OMe-dG10@N7	dG6@N2	5.64	OMe-dG11@O6	dG14@N1	49.64
OMe-dG10@O6	dG6@N1	22.45	dG5@N7	OMe-dG11@N2	0
dG15@N1	OMe-dG10@N2	0	dG2@O6	dG5@N1	0
dG1@O6	dG15@N1	0	dG2@N7	dG5@N2	0
dG1@N7	dG15@N2	0	dG14@O6	dG2@N1	0
dG6@N7	dG1@N2	0	dG5@O6	OMe-dG11@N1	25.20
dG6@O6	dG1@N1	0	dG14@N7	dG2@N2	0

definitely smaller value 23.90%. In light of the protection of TGT loop, the hydrogen bonds formed by the dG10 and dG6 are more stable than the others during the native unfolding process [28]. However, G4-quartet-A is less stable than G4-quartet-B by comparing existence percentages and numbers of Hoogsteen hydrogen bonds. Collectively, these evidences demonstrated that 2′OMe-G10 led to a significant destabilization effect than 2′OMe-G11 on the G4 structure.

3.4. Dihedral angle analysis

The flexibility of phosphor backbone of the nucleic acid is a

critical structure parameter to measure and describe the backbone torsional mobility of the G4 structure [29]. Therefore, we also analyzed the following two dihedral angles: one dihedral (C3′–O3′–P–O5′) in the 5′ direction as G4-A and the other one (P–O5′–C5′–C4′) as G4-B. As shown in Fig. 2A, the distribution of the G4-A dihedral exhibits a main peak around 285° and a secondary peak at 85°, respectively, with some minor peaks distributed along with the two peaks. Obviously, this structural feature confers more flexibility to the phosphor backbone of G4-quartet-A and significantly decreases the stability of G4 structure. With respect to the G4-B dihedral (Fig. 2B), although some minor peaks were observed, the main peak was still around 180° corresponding to the native distribution and no obvious secondary peak was detected. Therefore, these results indicated that the 2′OMe-G11 has minor effects on the phosphor backbone of G4-quartet-B. According to the dihedral angle analysis results, albeit both 2′OMe-G10 and 2′OMe-G11 increase the flexibility of TBA G4 quartets, we can infer that 2′OMe-G10 has more destabilization effects on the TBA G4 structure than 2′OMe-G11.

3.5. Glycosyl torsion angle analysis

The glycosyl torsion angle describes the relative glycosyl orientation: syn conformation possesses a specific angle distribution (0°–90°), while anti conformation has another preference range (180°–360°). It is well known that the glycosidic conformational patterns of the guanines forming the G-quartets have important effects on the formation, stability or folding topology of the G4 [30]. For TBA aptamer, all the guanines on the same G-quartet adopt alternating syn/anti conformations [31]. According to all the published structures, guanine at position 10 adopts a syn conformation, while an anti conformation is necessary for the guanine at position 11 [9,28]. Previously, we also investigated the structure stability of TBA by classical MD simulation and obtained plenty of structural information [25,26]. In order to further inquire the destabilized factors, we thus analyzed the biased glycosyl torsion angle of 2′OMe-G10 and 2′OMe-G11 by comparing with our previous classical MD results.

As illustrated in Fig. 3A, the glycosyl torsion angle distribution of 2′OMe-G10 at 300 K showed a single peak ranging from 20° to 100° which represents a syn conformation, but in comparation with dG10, the average value is increased. As for the 2′OMe-G11 (Fig. 3B), continuous double peaks were observed, but the distribution of angle ranges were all within the anti conformation. Clearly, 2′OMe-G modification makes the glycosyl torsion angle of 2′OMe-G10 and 2′OMe-G11 more flexibility. Although we have observed some variations of distribution, the large conformation transition has not been captured at 300 K.

In order to further probe the effects of 2′OMe-G10 and 2′OMe-G11, we analyzed the glycosyl torsion angle distributions at a higher temperature (375 K). Interestingly, the glycosyl torsion angle distributions of 2′OMe-G10 (Fig. 3C) and 2′OMe-G11 (Fig. 3D) at 375 K displayed double peaks: a main peak around 285° and the other minor peak is around 40 °, corresponding to an anti-conformation. It is noted that all the glycosyl torsion angle of 2′OMe-G10 displayed anti-conformation, which is converse to the dG at position 10 in native TBA. In contrast, 2′OMe-G11 kept an anti conformation in the two different temperatures. Obviously, the dominant conformation of 2′OMe-G10 is not a syn conformation which is necessary for the TBA G4 structure. It is well known that the anti and syn conformation transition needs to conquer a large energy barrier, which is unfavorable for the folding process. Thus, we can infer that the anti glycosyl conformation of 2′OMe-G10 is a major impediment for the folding and stability of mTBA G4 structure.

3.6. Sugar pucker analysis

The furanose ring in nucleic acids is conformationally flexible and the sugar pucker describes the extent to by which the furanose ring in nucleic acids deviates from a plane. Sugar conformation usually defined as sugar pucker, either an RNA-like C3′-endo (North, N) conformation or a DNA-like C2′-endo (South, S) conformation, is also a valuable parameter to characterize the nucleic acid structure [31]. Normally, S conformation possesses a specific angle distribution: 140 °–185 ° and N conformation has another preference range: (−10 °) –40 °.

In order to avoid the steric repulsion, modified nucleotides usually favored a certain type of sugar pucker. More importantly, these sugar puckers are related to different glycosyl conformation. Due to the steric consequences introduced by the modification group, the N conformation rather disfavors the syn glycosyl orientation, but the anti-conformation is not so sensitive to the sugar pucker [31]. In order to inquire the impacts of the 2′OMe-G modifications on the G4 structure, we carried out the sugar pucker

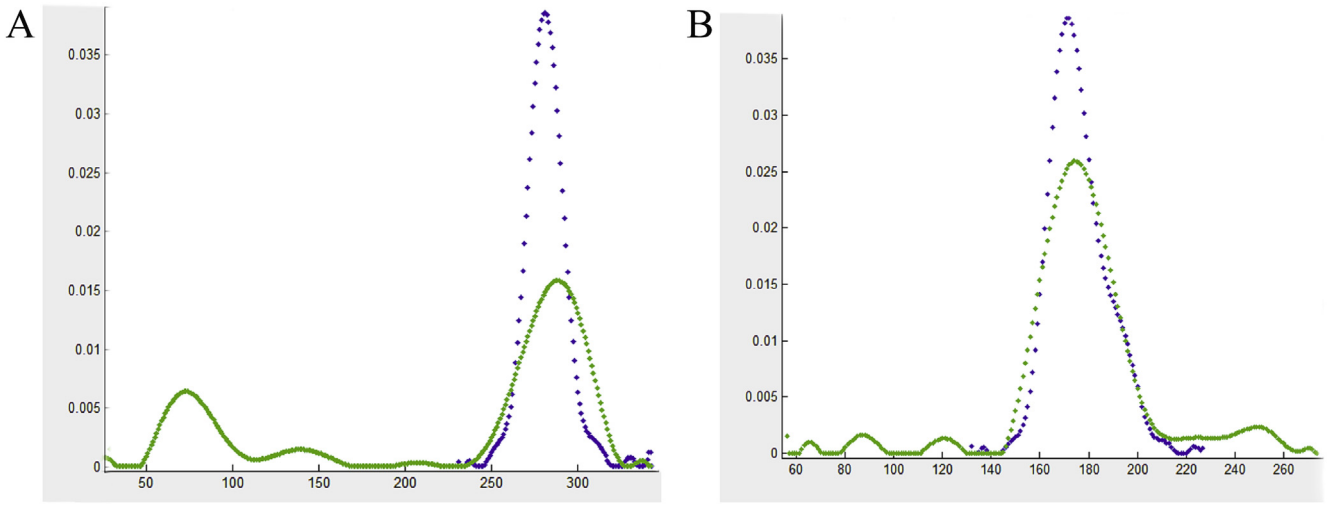

Fig. 2. The probability density distributions of the selected backbone dihedrals calculated over the whole production runs. A. G4-A; B. G4-B. The purple line and the green line represent the native TBA and mTBA, respectively. (For interpretation of the references to colour in this figure legend, the reader is referred to the Web version of this article.)

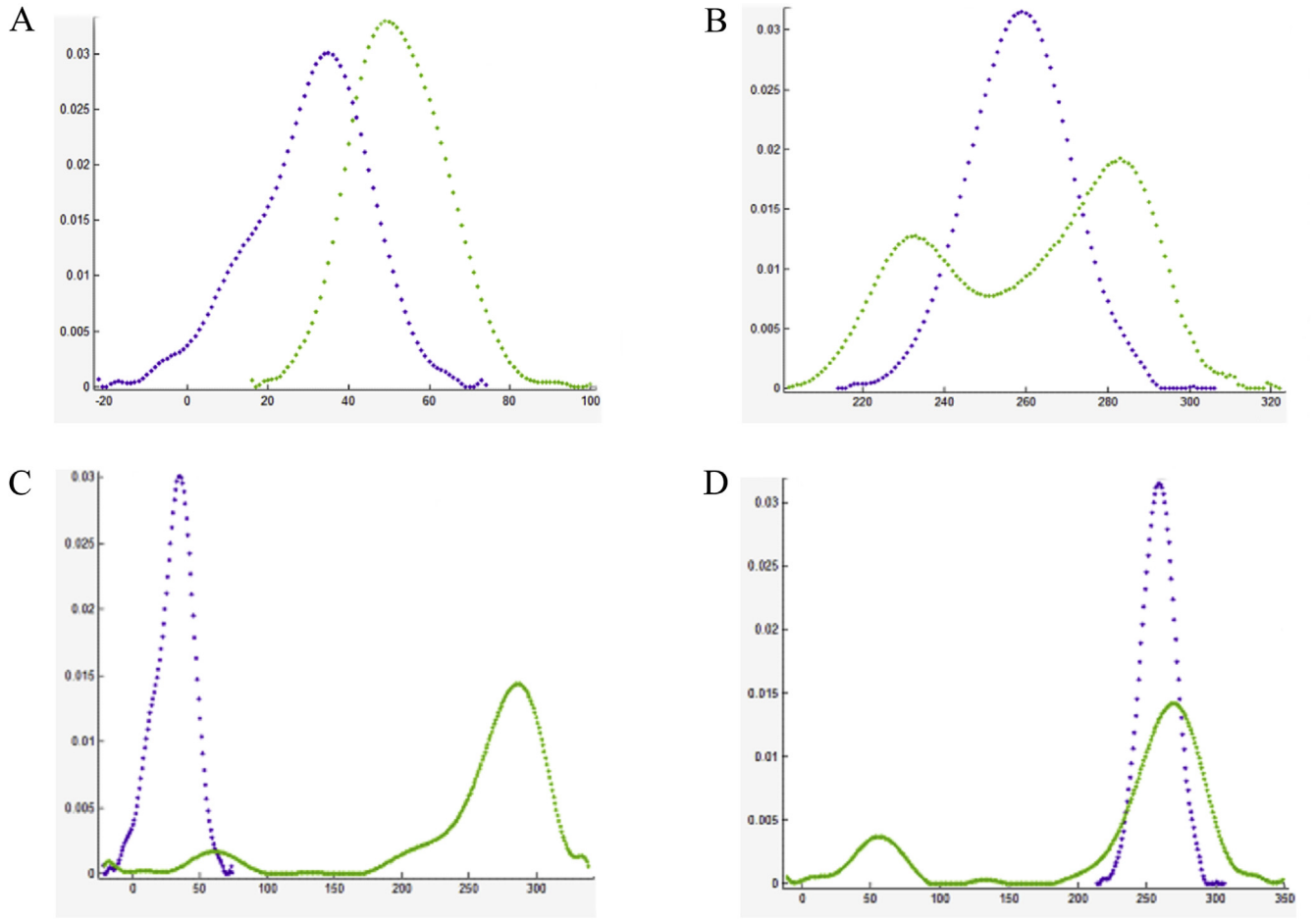

Fig. 3. The distributions of glycosyl torsion angle of 2′OMe-G10 and 2′OMe-G11 at 300 K and 375 K. A. 2′OMe-G10 at 300 K; B. 2′OMe-G11 at 300 K; C. 2′OMe-G10 at 375 K; A. 2′OMe-G11 at 375 K.

analysis especially on the 2′OMe-G10 and 2′OMe-G11.

As shown in Fig. 4A and B, the distributions exhibited two peaks, a main peak around 180° and the other one is around 40°, corresponding to S conformation and N conformation, respectively. The conformational distribution of 2′-dG in the two G-quartets of the TBA aptamer is well defined and all sugar puckers are S conformations [31]. In comparation with S conformation, N conformation is not favorable for the folding process and will decrease the stability of TBA G4 structure. As we have mentioned above, 2′OMe-G11 adopts an anti glycosyl conformation which is not sensitive to the sugar pucker, suggesting that the introduction of the 2′OMe-G at position 11 has small negative structural impacts.

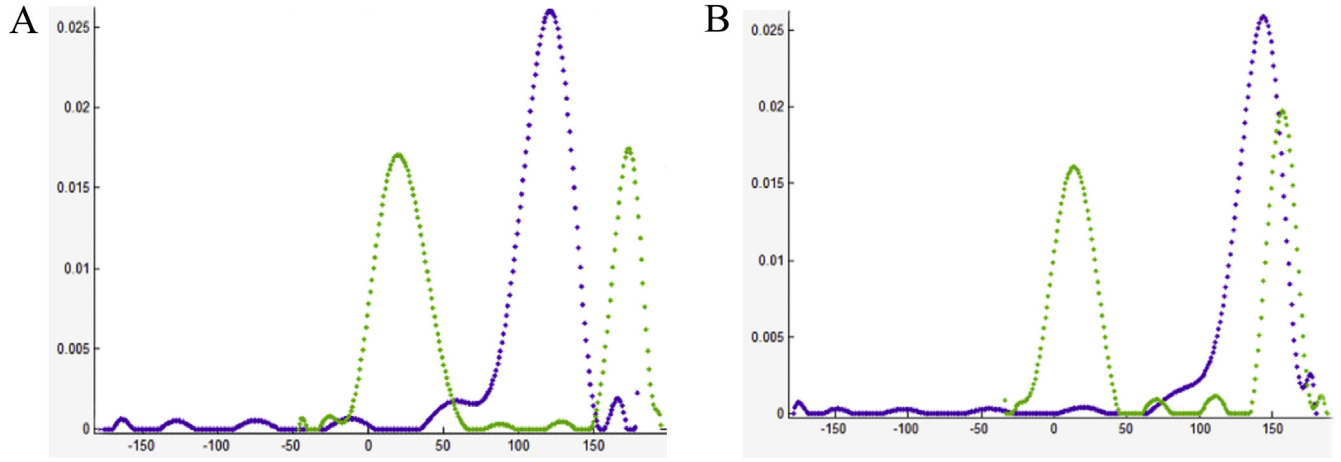

Fig. 4. The probability density distributions of sugar pucker of 2′OMe-G10 and 2′OMe-G11. A. 2′OMe-G10; B. 2′OMe-G11.

However, N conformation of 2′OMe-G10 strongly disfavors the syn conformation which is necessary for the formation of G4 structure. Clearly, in order to fold into a native-like TBA G4 structure, the 2′OMe-G10 has to change its native anti conformation and maintain the syn/N conformation that is not supported on the steric and energy aspects. These results also can explain why the 2′OMe-G10 preferred to exist as an anti conformation. As for 2′OMe-G11, it does not require to change glycosyl conformation and easily adopt the essential conformation for the folding process. Collectively, these distributions demonstrated that mTBA can't fold into a native-like G4 structure and the N conformation of 2′OMe-G10 is also a major interfering factor.

Conflicts of interest

The authors have no conflicts of interest.

Acknowledgements

This work was supported by the National Natural Science Foundation of China (Grant No. 21502104).

Appendix A. Supplementary data

Supplementary data to this article can be found online at https://doi.org/10.1016/j.bbrc.2019.09.065.

References

[1] S. Burge, G.N. Parkinson, P. Hazel, A.K. Todd, S. Neidle, Quadruplex DNA: sequence, topology and structure, Nucleic Acids Res. 19 (2006) 5402–5415.
[2] C.K. Kwok, C.J. Merrick, G-Quadruplexes, Prediction, characterization, and biological application, Trends Biotechnol. 35 (2017) 997–1013.
[3] G.W. Collie, G.N. Parkinson, The application of DNA and RNA G-quadruplexes to therapeutic medicines, Chem. Soc. Rev. 40 (12) (2011) 5867–5892.
[4] D. Yang, G-Quadruplex DNA and RNA, Methods Mol. Biol. 2035 (2019) 1–24.
[5] S. Zhang, Y. Wu, W. Zhang, G-quadruplex structures and their interaction diversity with ligands, ChemMedChem 9 (201) (2014) 899–911.
[6] J. You, H. Li, X.M. Lu, W. Li, P.Y. Wang, S.X. Dou, X.G. Xi, Effects of monovalent cations on folding kinetics of G-quadruplexes, Biosci. Rep. 37 (2017) pii: BSR20170771.
[7] M. Sharawy, S. Consta, Effect of the chemical environment of the DNA guanine quadruplex on the free energy of binding of Na and K ions, J. Chem. Phys. 149 (2018), 225102.
[8] L.C. Bock, L.C. Griffin, J.A. Latham, et al., Selection of single-stranded DNA molecules that bind and inhibit human thrombin, Nature 355 (1992) 564–566.
[9] I. Russo Krauss, A. Merlino, A. Randazzo, E. Novellino, L. Mazzarella, F. Sica, High-resolution structures of two complexes between thrombin and thrombin-binding aptamer shed light on the role of cations in the aptamer inhibitory activity, Nucleic Acids Res. 40 (2012) 8119–8128.
[10] I. Russo Krauss, A. Merlino, C. Giancola, A. Randazzo, L. Mazzarella, F. Sica, Thrombin-aptamer recognition: a revealed ambiguity, Nucleic Acids Res. 39 (2011) 7858–7867.
[11] G. Ying, X. Lu, J. Mei, Y. Zhang, J. Chen, X. Wang, Z. Ou, Y. Yi, A structure-activity relationship of a thrombin-binding aptamer containing LNA in novel sites, Bioorg. Med. Chem. 27 (2019) 3201–3207.
[12] X.Y. Zhao, B. Liu, J. Yan, Y. Yuan, L.W. An, Y.F. Guan, Structure variations of TBA G-quadruplex induced by 2' -O-methyl nucleotide in K^{+} and Ca^{2+} environments, Acta Biochim. Biophys. Sin. 46 (2014) 837–850.
[13] A. Pasternak, F.J. Hernandez, L.M. Rasmussen, B. Vester, J. Wengel, Improved thrombin binding aptamer by incorporation of a single unlocked nucleic acid monomer, Nucleic Acids Res. 39 (2011) 1155–1164.
[14] B.B. Cai, X.T. Yang, L.D. Sun, X.M. Fan, L.Y. Li, H.W. Jin, Y. Wu, Z. Guan, L.R. Zhang, L.H. Zhang, Z.J. Yang, Stability and bioactivity of thrombin binding aptamers modified with D-/L-isothymidine in the loop regions, Org. Biomol. Chem. 12 (2014) 8866–8876.
[15] B. Okumus, T. Ha, Real-time observation of G-quadruplex dynamics using single-molecule FRET microscopy, in: G-quadruplex DNA: Methods and Protocols, vol. 608, 2010, pp. 81–96.
[16] C.G. Peng, M.J. Damha, G-quadruplex induced stabilization by 2'-deoxy-2'-fluoro-D-arabinonucleic acids (2'F-ANA), Nucleic Acids Res. 35 (2017) 4977–4988.
[17] Q. Tang, X. Su, K.P. Loh, Surface plasmon resonance spectroscopy study of interfacial binding of thrombin to antithrombin DNA aptamers, J. Colloid Interface Sci. 315 (2007) 99–106.
[18] C.M. Olsen, L.A. Marky, Monitoring the temperature unfolding of G-quadruplexes by UV and circular dichroism spectroscopies and calorimetry techniques, in: G-quadruplex DNA: Methods and Protocols, vol. 608, 2010, pp. 147–158.
[19] S. Haider, S. Neidle, Molecular modeling and simulation of G-quadruplexes and quadruplex-ligand complexes, Methods Mol. Biol. 608 (2010) 17–37.
[20] X.M. Fan, L.D. Sun, Y. Wu, L.H. Zhang, Z.J. Yang, Bioactivity of 2'-deoxyinosine-incorporated aptamer AS1411, Sci. Rep. 6 (2016) 25799.
[21] X.M. Fan, L.D. Sun, K.F. Li, X.T. Yang, B.B. Cai, Y.F. Zhang, Y.J. Zhu, Y. Ma, Z. Guan, Y. Wu, L.H. Zhang, Z.J. Yang, The bioactivity of D-/L-Isonucleoside- and 2'-deoxyinosine-incorporated aptamer AS1411s including DNA replication/microRNA expression, Mol. Ther. Nucleic Acids 9 (2017) 218–229.
[22] T.Q. Yu, J. Lu, C.F. Abrams, E. Vanden-Eijnden, Multiscale implementation of infinite-swap replica exchange molecular dynamics, Proc. Natl. Acad. Sci. U.S.A. 113 (2016) 11744–11749.
[23] C. Yang, M. Kulkarni, M. Lim, Y. Pak, In silico direct folding of thrombin-binding aptamer G-quadruplex at all-atom level, Nucleic Acids Res. 45 (2017) 12648–12656.
[24] P. Stadlbauer, M. Krepl, T.E. 3rd Cheatham, J. Koca, J. Sponer, Structural dynamics of possible late-stage intermediates in folding of quadruplex DNA studied by molecular simulations, Nucleic Acids Res. 41 (2013) 7128–7143.
[25] L.D. Sun, H.W. Jin, X.Y. Zhao, Z.M. Liu, Y.F. Guan, Z.J. Yang, L.R. Zhang, L.H. Zhang, Unfolding and conformation variations of Thrombin-binding DNA aptamer: synthesis, circular dichroism and molecular dynamics simulations, ChemMedChem 9 (5) (2014) 993–1001.
[26] L.D. Sun, X.L. Xie, W.T. Weng, H.W. Jin, Structural and mechanistic insights into modified G-quadruplex thrombin-binding DNA aptamers, Biochem. Biophys. Res. Commun. 513 (2019) 753–759.
[27] S. Kannan, M. Zacharias, Simulation of DNA double-strand dissociation and formation during replica-exchange molecular dynamics simulations, Phys. Chem. Chem. Phys. 11 (2019) 10589–10595.
[28] X. Mao, W.H. Gmeiner, NMR study of the folding-unfolding mechanism for the thrombin-binding DNA aptamer d(GGTTGGTGTGGTTGG), Biophys. Chem. 113 (2005) 155–160.
[29] M. Cavallari, A. Garbesi, R. Di Felice, Porphyrin intercalation in G4-DNA quadruplexes by molecular dynamics simulations, J. Phys. Chem. B 113 (2009) 13152–13160.
[30] X. Cang, J. Šponer, T.E. 3rd Cheatham, Explaining the varied glycosidic conformational, G-tract length and sequence preferences for anti-parallel G-quadruplexes, Nucleic Acids Res. 39 (2011) 4499–4512.
[31] H. Saneyoshi, S. Mazzini, A. Aviñó, G. Portella, C. González, M. Orozco, V.E. Marquez, R. Eritja, Conformationally rigid nucleoside probes help understand the role of sugar pucker and nucleobase orientation in the thrombin-binding aptamer, Nucleic Acids Res. 37 (2009) 5589–5601.